J. Min. Metall. Sect. B-Metall. 48 (1) B (2012) 309 - 318

Journal of Mining and Metallurgy

PREPARATION, CHARACTERIZATION AND MECHANICAL PROPERTIES OF RARE-EARTH-BASED NANOCOMPOSITES

S.S. Musbah[*], V. Radojević[*], I. Radović[*], P.S. Uskoković[*], D.B. Stojanović[*], M.Dramićanin[**], R. Aleksić[*,#]

[*]University of Belgrade, Faculty of Technology and Metallurgy, Belgrade, Serbia
[**]University of Belgrade, Institute of Nuclear Sciences "Vinča", Belgrade, Serbia

(Received 08 May 2012; accepted 04 June 2012)

Abstract

This study reports research related to different preparation methods and characterization of polymer nanocomposites for optical applications. The Eu-ion doped Gd_2O_3 nanophosphor powder with different nanoparticle content was embedded in the matrix of PMMA. Preparation was carried out by mixing molding (bulk), electrospinning (nanofibers) and solution casting (thin films) with neat particles and particles coated with AMEO silane. Among the pros and cons for proposed methods, the mixing molding enables to avoid solvent use while the best deagglomeration and nanoparticle distribution is gained using the electrospinning method. The results of dynamic mechanical analysis (DMA) and nanoindentation revealed that the storage modulus of the composites was higher than that of pure PMMA and increased with nanophosphor content. Surface modification of particles improved the mechanical properties of nanocomposites.

Keywords: Nanocomposites; Nanophosphors; Electrospinning; Dynamic mechanical analysis; Nanoindentation

1. Introduction

Rare-earth-based nanoparticles are highly photostable and exhibit long luminescence lifetimes and narrow emission bands with similar properties as those of quantum dots [1]. They possess excellent luminescent properties of inorganic phosphors which lead to promising applications of polymer – nanophosphor composites. Among the inorganic oxides, Gd_2O_3 [2-5] was widely employed as ideal host materials for the rare

[#] *Corresponding author: aleksic@tmf.bg.ac.rs*

DOI:10.2298/JMMB120508030M

earth ions (RE) ion down- or up-conversion emission because of their low-phonon energy, high chemical- and photo stability, and efficient sensitization (host-to- RE energy transfer).

Thermoplastic polymer nanocomposites doped with the rare earth ions such as Tb, Eu, Yb and Er have attracted considerable interest due to energy transfer, up-conversion effects and broad application possibilities. They have a wide range of applications in photonic devices, signal links in medical devices, illuminating systems, fiber optic sensors and amplifiers [6-9]. Recently, polymer optical fibers have found new applications in bio-sensors, bio-analytics and even clinical imaging diagnostics.

Poly (methyl methacrylate) (PMMA) is known as an optical plastic with excellent transparency and good processability, but with relatively poor mechanical properties. For improvement of mechanical properties of the transparent PMMA, techniques are used such as polymer blending and nanoparticles or continuous fiber reinforcement [10-13]. As a consequence, the transmittance of the composites decreased significantly due to the difference between refractive indices of the PMMA and the reinforcement materials. An imperfect interface also contributes to the composite opacity. To resolve these problems, a potential method is to reduce the diameter of the reinforcing fibers to a size smaller than the wave-length of a visible light, so that the visible light does not reflect or refract while travelling through the composite [14]. Selected nanophosphors satisfy the prerequisites for presented hypothesis in that the size of particles in optical composites should be less than the wavelength of light because of light scattering and the appropriate deagglomeration of nanoparticles in composite preparation could lead to the increase of mechanical properties. The optical effectiveness of the Eu:Gd_2O_3 in PMMA has already been reported [15, 16].

The melt mixing molding is quite extensive composite processing technique, with the pros and cons in that there is no need for other chemicals as for solution methods, but the deagglomeration and dispersion degree, especially in nano dimension, is rather low in comparison to other processing routes.

Solution casting method is usually utilized for processing of polymer nanocomposites because of the wide possibilities in mixing and deagglomeration of nanoparticles in solution. Potential drawbacks emerge with forming films after casting, with their thickness and particle distribution uniformity. Some of them could be resolved using the spin coating method.

Electrospinning is a versatile and effective technique to produce long, continuous fibers, and it is applicable to a diversity of materials, including not only polymers, [17-19] but also bio-molecules, [20, 21] as well as inorganic/polymer composites [22-24]. It is an electrostatically induced assembly process for generating ultrathin fibers with nanoscale diameters.

Thermo-mechanical properties of nanocomposites in form of bulk, films or nanofibers were measured by DMA because this technique is able to detect short range motion before the glass transition range is attained and thus identify the onset of main chain motion. Thus, the DMA method is

more sensitive to detection of temperature transition than DSC because the mechanical changes are more dramatic than changes in the heat capacity [25, 26]. In addition, the nanomechanical properties of composite films were measured in order to point the effects of silanization of nanoparticles.

2. Experimental

Commercially available PMMA Acryrex® CM205 (Chi Mei Corp.) pellets were used as a matrix for preparing samples (Mw≈90400 g/mol). The Gd_2O_3 doped with 3 at. % Eu^{3+} nanopowder was synthesized using the combustion reaction based on polyethylene glycol (PEG) fuel [15]. The particle size of the Eu:Gd_2O_3 sample was determined by transmission electron microscopy-TEM (Phillips CM100 instrument operating at 60 kV). The silane coupling agent used for modification of particles was γ-Aminopropyltriethoxysilane- AMEO, Dynasylan® Evonik-Degussa [27]. In the present study, the grafting reaction was carried out in a 95 wt% ethanol - 5 wt% water mixture to yield a 2 wt% final concentration of silane. The required amount of AMEO silane was calculated assuming 1 mol of AMEO per mol of Eu:Gd_2O_3. After silane addition the dispersion was refluxed with intensive stirring for 48 h at 80 °C, centrifuged and washed with ethanol in order to remove the residual silane and dried at 110 °C in a vacuum oven. Bulk nanocomposites were produced using Laboratory mixing molder, Dynisco. The sample contents were processed with different Eu:Gd_2O_3 powder: 0.5 wt%; 1.0 wt%: and 3 wt%. Nanocomposite films and nanofibers were processed with content of 3 wt% of unmodified and modified particles. Three solutions with fixed polymer concentration at 22 wt% were made using dimethylformamide (DMF, Uvasol® for spectroscopy, Merck-Alkaloid, Skopje) as solvent. The first solution was used for preparation of film and electrospun nanofibers of pure PMMA. The second solution consisted of polymer and Eu:Gd_2O_3 particles and the third contained polymer and AMEO modified Eu:Gd_2O_3 particles. Concentration of particles was set as 3 wt% related to polymer. One part of solution was used for electrospinning and the other was for solution casting. Electrospinning process (Electrospinner CH-01, Linari Engineering, Italy.) was setup: a 20 ml plastic syringe with a metallic needle of 1 mm inner diameter was set vertically on the syringe pump (R-100E, RAZEL Scientific Instruments); the high-voltage power supply (Spellman High Voltage Electronics Corporation, Model: PCM50P120) was set to the voltage of 28 kV. The flow rate of polymer solution was constant at 0.5 ml/h. Distance from the needle tip and collector was 14 cm. For the solution casting the solutions were poured into flat-bottomed Petri dishes to form film with a thickness of 500 μm. The infrared (IR) spectra of samples in KBr discs were obtained by transmission Fourier transform infrared (FTIR) spectroscopy (Hartmann & Braun, MB-series). The FTIR spectra were recorded between 4000 and 400 cm^{-1} with a resolution of 4 cm^{-1}. An insight of dispersion and deagglomeration of nanoparticles was performed using FESEM (TESCAN MIRA 3) with fracture surfaces sputtered with gold. The measuring of electrospun nanofibers

diameter was performed by Image Pro Plus 4.0. A dynamic mechanical analyzer DMA Q800 (TA Instruments) was used in the dual cantilever mode over a temperature range from 25 °C to 160 °C at a fixed frequency of 1 Hz. The heating ramp rate was 3 °C/min. DMA of fibers and thin films was established with the stainless steel sample holder loaded in the DMA Q800 (TA Instruments) using a dual cantilever mode, with temperature ramp 3 °C/min from 30 °C to 160 °C, and at a fixed frequency of 1 Hz. Because of the architecture of electrospun nanofibers, the modified DMA tests were performed with specific stainless steel sample holder with the 60 mm×13 mm×1 mm dimensions [26].

Nanoindentation tests on the polymer and composite film samples were done using the Hysitron Triboindenter with a Berkovich diamond tip and in-situ imaging scan mode. The hardness and reduced elastic modulus were calculated from the curves using the Oliver and Pharr method [28]. The indentation maximum load was set to be 2 mN for all tested samples. The loading and unloading times as well as the hold time at the peak force were set to 25 s each.

3. Results and discussion

Morphology and particle sizes of powder were checked with TEM. It is revealed that Eu:Gd_2O_3 nanopowders in the form of particle agglomerates with dimensions of individual particles of about 40 nm, as shown in Figure 1.

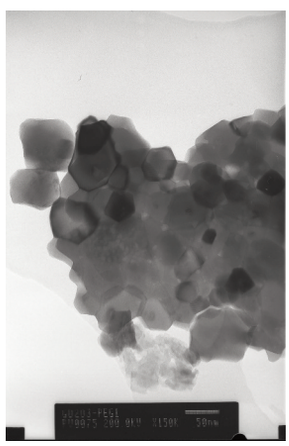

Figure 1. TEM image of Eu: Gd_2O_3 powder

FESEM photos of the composite fracture surfaces of bulk samples and films with unmodified (a) and modified (b) particles are presented in Figures (2-3). FESEM analysis

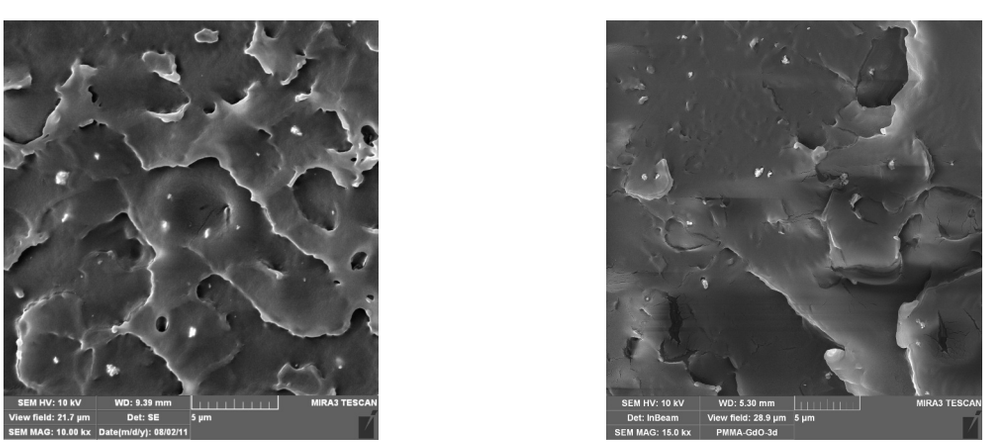

Figure 2. FESEM of bulk samples: a) PMMA-Eu:Gd_2O_3 (3 wt %); b) PMMA-Eu:Gd_2O_3-AMEO (3 wt %)

reveals that the better dispersion of nanoparticles is achieved with modified particles. The silanization of particles leads to better deaglomeration of particles.

SEM photos of the electrospun nanofibers are presented in Figure 4. Image analysis revealed that nanofibers were in mean diameter of 200-500 nm of PMMA, 400-600 nm of PMMA-Eu:Gd_2O_3 and 300-550 nm of PMMA-Eu:Gd_2O_3-AMEO nanocomposites, respectively. A favorable dispersion of particles in nanofibers was achieved and a better deaglomeration of modified particles was obtained.

The FTIR spectrum of unmodified, modified Eu:Gd_2O_3 nanoparticles and AMEO silane is presented in Figure 5. The IR spectrum of unmodified Eu:Gd_2O_3 shows

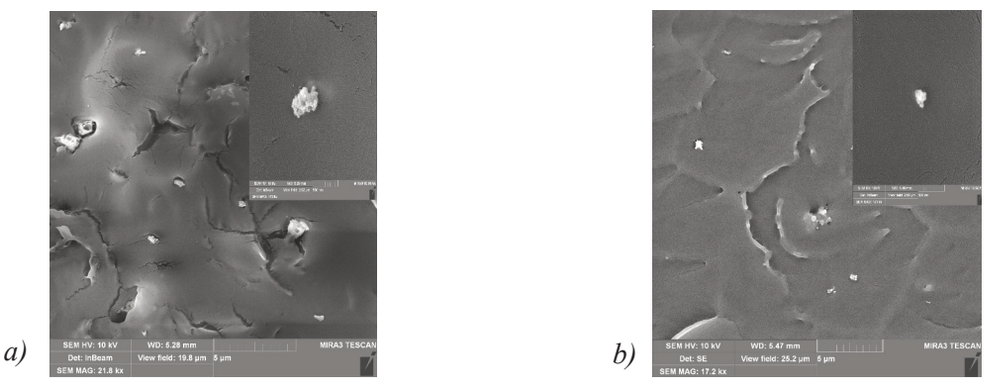

Figure 3. FESEM photos of films: a) PMMA-Eu:Gd_2O_3 (3 wt %); b) PMMA-Eu:Gd_2O_3-AMEO (3 wt %)

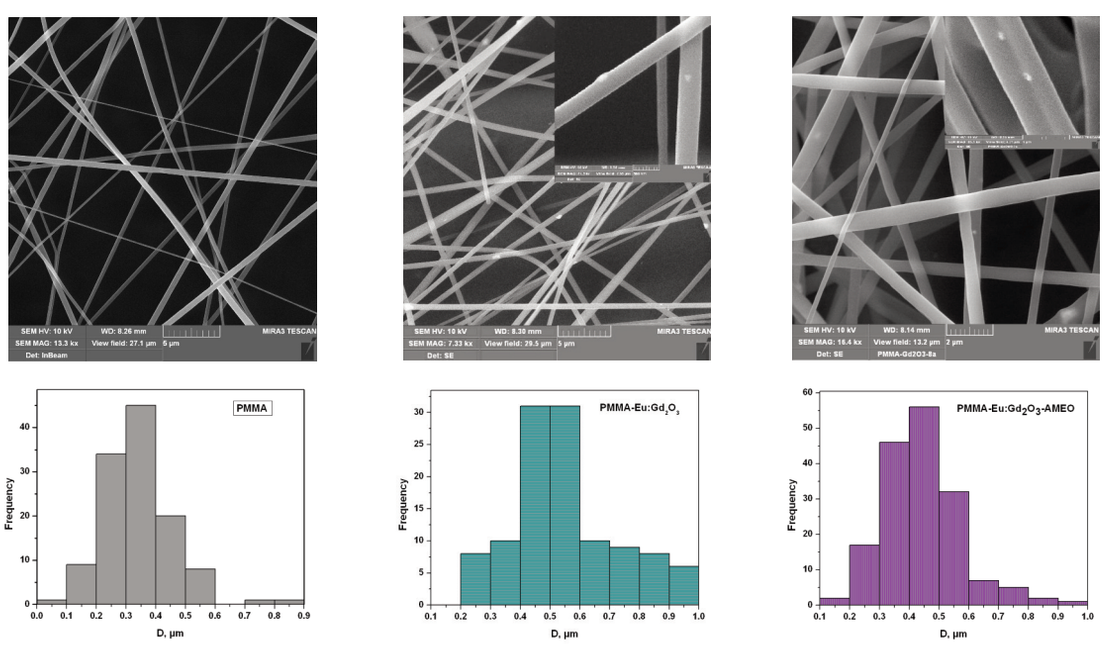

Figure 4. FESEM photo of electrospun nanofibers: a) PMMA; b) PMMA-Eu:Gd_2O_3 (3 wt%); c) PMMA-Eu:Gd_2O_3-AMEO (3 wt %)

the characteristic bands observed at 1017, 1397 and 1506 cm^{-1} of nitrate and carbonate as consequence of combustion method [29]. The presence of adsorbed water molecules is assigned to the bands $\delta(H_2O)$ at 1635 cm^{-1} and $\nu(H_2O)$ at 3434 cm^{-1}. The characteristic band for Gd-O bond is observed at 542 cm^{-1}. The FTIR spectrum of the amino modified gadolinium particles (Figure 5 (b)), shows the band originating from Si-O-Si vibrations at 1064 cm^{-1}, and the weak bands at 2924 cm^{-1} and 2846 cm^{-1}, which were assigned to the asymmetric, ν_{as}, and symmetric, ν_s, stretching modes of CH_2 groups. In the FTIR spectrum of the amino modified gadolinium particles, Figure 5 (b), can be seen the band originating from Si-O-Si vibrations at 1064 cm^{-1}, the weak bands at 2924 cm^{-1} and 2846 cm^{-1} were assigned to the asymmetric, ν_{as}, and symmetric, ν_s, stretching modes of CH_2 groups. The band at 1128 cm^{-1} could also be due to Si-O-Gd groups, the weak band at 1541 cm^{-1} may be attributed to $\delta(NH_2)$ deformation vibrations of the NH_2 groups, respectively, which is in agreement with the data reported in the literature [27]. The broadening of the signal centered at about 3434 cm^{-1} was also assigned to the presence of adsorbed water molecules and overlapped with signals of $\nu(H_2O)$ of the adsorbed water, silanol and $\nu(NH_2)$ group vibrations. This indicates that the chemical modification on $Eu:Gd_2O_3$ surface was achieved.

Further investigation on the optimal composite configuration for appropriate mechanical properties was undertaken by DMA, as presented in Figure 6. The results of DMA for bulk samples with different nanophosphors are presented in Figure 6 (a). The glass transition temperature (T_g) of a polymer increased after the addition of inorganic fillers and the storage modulus composites are changed correspondingly [30]. It is obvious that even in the absence of specific interactions with the polymer, the particles behaved as functional physical crosslink and thus reducing the overall mobility of the polymer chains, as was already reported [31, 32]. After adding the modified particles, the storage modulus increased considerably and T_g increased slightly (Figure 6 (b)). So, the modification of interface particle-matrix improved the mechanical properties of nanocomposite.

The using of stainless steel holder enabled the characterization of the T_g with temperature change by observing the signal change of the calculated normalized complex modulus, E^* [25-26, 33-35]. The magnitudes of the storage modulus and the loss modulus are only qualitative. This complex modulus, E^*, presents the ratio of the complex modulus within a sample set to the value of the maximum modulus in the same data set. The DMA results for nanofibers (Figure 6 (c)) clearly display that the glass transition temperature is accompanied by significant

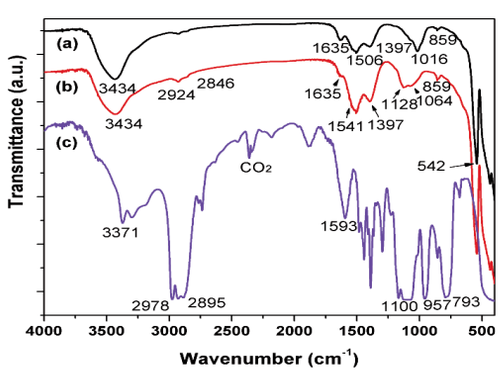

Figure 5. The FTIR spectrum of a) neat $Eu:Gd_2O_3$, b) modified $Eu:Gd_2O_3$ and c) AMEO silane

loss (onset point) of the normalized complex modulus, E^*. Better thermal stability was achieved for nanocomposite with modified particles with respect to nanocomposite with unmodified particles and pure PMMA. The shift of T_g for nanofibers is more remarkable than that for bulk samples. This indicates that the distribution of nanoprticles is much better in electrospun nanofibers. DMA results for films with modified and unmodified particles obtained by steel sample holder are presented in Figure 6 (d). The results show that the onset point, corresponding to the α-transition (glass transition), is shifted towards the lower temperatures, as compared with the bulk polymer obtained by molding, without any solvent. The effect of the solvent contained in the film decreases the glass transition temperature (T_g) of the polymer and composites [36, 37]. But the results show the same trend as a bulk and nanofibers in that the value of T_g raised in the order PMMA, PMMA-Eu:Gd_2O_3 and PMMA-Eu:Gd_2O_3-AMEO.

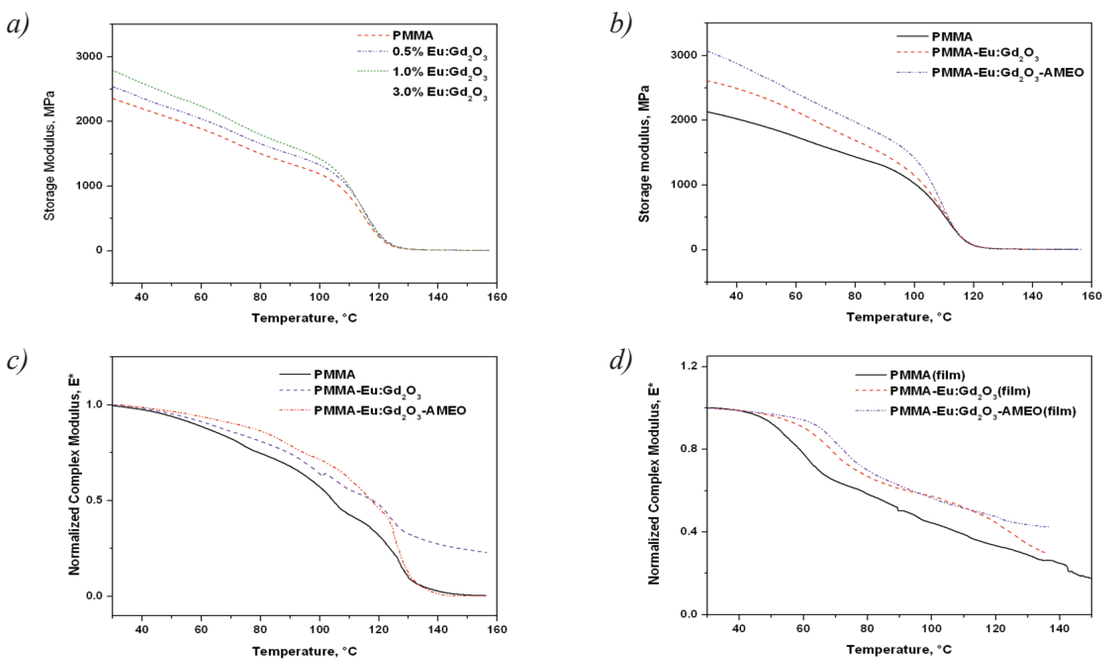

Figure 6. DMA- a) Storage modulus of pure PMMA and nanocomposites- Bulk samples; b) Storage modulus of pure PMMA and nanocomposites with 3 wt% unmodified and 3 wt% modified nanoparticles; c) Complex modulus, E, of electrospun nanofibers; d) Complex modulus, E*, of different films*

Table 1. Temperature transformation, T_g, for bulk samples, nanofibers and films obtained from DMA

Sample	T_g/° C Bulk samples	T_g/° C Nanofibers	T_g/° C Films
PMMA	101.18	97.47	60.02
PMMA-Eu:Gd_2O_3	101.76	102.89	62.31
PMMA-Eu:Gd_2O_3-AMEO	102.12	107.68	64.12

Figure 7 (a) shows typical force–depth curves obtained in the nanoindentation tests for neat PMMA film and composites with Eu:Gd_2O_3 and AMEO silane treated Eu:Gd_2O_3. The curves appear to be with continuity and without pop in or pop out in both loading and unloading phases. Figure 7 (b) displays the plastic imprint of the indent for the sample with AMEO silane treated particles with the scan trace in the vicinity of the indent. In-situ imaging mode used for scanning the surface trace reveals the absence of cracks and fractures around the indent. Line trace shows small piling-up along the edges but in addition to the film surface roughness (adequate but not ideal); these scans (only one is displayed) raise the confidence that nanoindentation tests captured actual material properties [38]. The results of reduced elastic modulus and hardness for neat polymer and composites with 3 wt% of nanoparticles are presented in Table 2. The reduced modulus for composite with untreated particles increases for 12.6% while the hardness remains similar in comparison to the neat PMMA films. For composites with AMEO silane treated particles the modulus increases for about 30% and hardness increase is about 11%. For composites with silane treated particles, results are comparable to those with other nanoparticle composites which achieved favorable dispersion and particle matrix bonding [39, 40]. Previous work reported the use of PEG silane, TEOS or grafting method for the silanization of Gd_2O_3 and RE:Gd_2O_3 nanoparticles [40, 41], this study presents the first report on the modification of Eu:Gd_2O_3 with AMEO silane adhesion promoter. The modification routes using PEG silane, TEOS or grafting methods leads to the appropriate nanoparticle deagglomeration in solvents (but not in polymer composites), as proven by electron microscopy and optical characterization of modified particles. This study presents the first attempt of

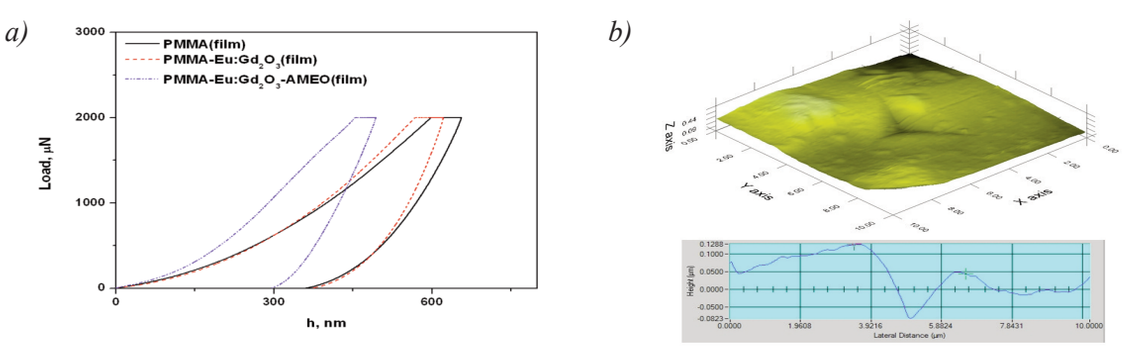

Figure 7. a) Load–displacement curves of neat PMMA and nanocomposite films; b) Indent plastic imprint with scan trace of the PMMA-Eu:Gd_2O_3-AMEO sample

Table 2. The results of nanoidentation, Elastic modulus and Hardness

Sample	E_r /GPa	Standard deviation/GPa	H/GPa	Standard deviation/GPa
PMMA	4.278	± 0.3	0.263	± 0.2
PMMA-Eu:Gd_2O_3	4.817	± 1.6	0.268	± 0.15
PMMA-Eu:Gd_2O_3-AMEO	5.597	± 1.0	0.293	± 0.15

establishing relations between the modification methods of Eu:Gd_2O_3 particles with the nanocomposite mechanical properties.

4. Conclusion

This study reports the preparation of composites with PMMA matrix reinforced with Eu:Gd_2O_3 nanophosphor powder with enhanced mechanical properties utilizing the quasi-industrial melt-mixing technique (bulk nanocomposite), solution casting (thin films) and electrospinnig (nanofiber). The three processing methods have different possibilities for the particle dispersion efficiency. The modification of the nanoparticles with the silane adhesion promotor enabled their dispersion and deagglomeration in all three cases (bulk, film and nanofibers) and yielded enhanced mechanical properties of the composite materials. The DMA results revealed that electrospinnig could be used for increased uniformity of nanoparticle distribution in polymer composites and that the relaxation temperatures associated with the glass transition (T_g) of the nanofibers were greater than those of the bulk and films nanocomposite samples. As shown by nanoindentation tests, incorporation of 3 wt% of silanized nanoparticles increased the reduced modulus and hardness of PMMA composite for 30% and 11% , respectively.

Acknowledgement

This work was supported by the Ministry of Education and Science of the Republic of Serbia, Projects No. TR 34011 and III 45019

References

[1] W. O. Gordon, J. A. Carter, B. M. Tissue, J. Lumin., 108 (2004) 339.

[2] Y. C. Kang, S. B. Park, I. W. Lenggoro, K. Okuyama, J. Phys. Chem. Solids, 60 (2000) 379.

[3] G. Xia, S. Wang, S. Zhou, J. Xu, Nanotechnology, 21 (2010) 345601.

[4] E. Ritzhaupt-Kleissl, J. Boehm, J. Hausselt, T. Hanemann. Mater. Sci. Eng. C, 26 (2006) 1067.

[5] X. Ye, W. Gao, L. Xia, H. Nie, W. Zhuang , J. Rare Earth., 28 (3) (2010) 345.

[6] R. M. Petoral, Jr., F. Söderlind, A. Klasson, A. Suska, M. A. Fortin, N. Abrikossova, L. Selegård, P.O. Käll, M. Engström, K. Uvdal, J. Phys. Chem. C, 113 (2009) 6913.

[7] T. K. Anh, P. Benalloul, C. Barthou, L. K. Giang, N. Vu, Le Quoc Minh., J. Nanomater., 2007 (2007) Article ID 48247, 10 pages, doi:10.1155/2007/48247

[8] R. J. Bartlett, R. Philip-Chandy, P. Eldridge, D. F. Merchant, R. Morgan, P. Scully, T. I. Meas. Control, 22 (5) (2000) 431.

[9] V. Radojević, T. Serbez, R. Aleksić, D. Nedeljković, Lj. Brajović J. Min. Metall. Sect. B-Metall, 41 B (1) (2005) 103.

[10] X. Wang, Z. Huang, L. Chen, Fiber. Polym., 12 (3) (2011) 359.

[11] S. K. Cheng, C. Y. Chen, Eur. Polym. J., 40 (2004) 1239.

[12] E. Schauer, L. Berglund, G. Pena, Polymer, 43 (2002) 1241.

[13] L. Q. Liu, D. Tasis, M. Prato, H. D. Wagner, Adv. Mater., 19 (2007) 1228.

[14] G. F. Chen, H. Q. Liu, J. Appl. Polym. Sci.,

110 (2008) 641.

[15] Z. Antic, R. Krsmanovic, M. Marinovic-Cincovic, M. D. Dramicanin. Acta Phys. Pol. A, 117 (2010) 831.

[16] M. Nichkova, D. Dosev, S. J. Gee, B. D. Hammock, I. M. Kennedy, Anal. Chem., 77 (2005) 6864.

[17] C. L. Casper, J. S. Stephens, N. G. Tassi, D. B. Chase, J. F. Rabolt, Macromolecules, 37 (2004) 573.

[18] K. P. Matabola, A. R. de Vries, A. S. Luyt, R. Kumar, Express Polym. Lett., 5 (7) (2011) 635.

[19] S. Piperno, L. Lozzi, R. Rastelli, M. Passacantando, S. Santucci, App. Surf. Sci., 252 (2006) 5583.

[20] Y. You, B. Min, S. J. Lee, T. S. Lee, W. H. Park, J. Appl. Polym. Sci., 95 (2005) 193.

[21] C. Hoffmann, A. C. Faure, C. Vancaeyzeele, S. Roux, O. Tillement, E. Pauthe, F. Goubard, Anal. Bioanal. Chem., 399 (2011) 1653.

[22] D. Li, Y. Xia, Adv. Mater., 16 (2004) 1151.

[23] J. Macossay, J. H. Leal, A. Kuang, R. E. Jones, Polym. Adv. Technol., 17 (2006) 391.

[24] M. Li, Z. Zhang, T. Cao, Y. Sun, P. Liang, C. Shao, Y. Liu, Mater. Res. Bull., 47 (2012) 321.

[25] D. Mahlin, J. Wood, N. Hawkins, J. Mahey, P. G. Royall, Int. J. Pharm. 371 (2009) 120.

[26] M. G. Abiad, O. H. Campanella, M. T. Carvajal, Pharmaceutics, 2 (2010) 78.

[27] A. M. Torki, D. B. Stojanović, I. D. Živković, A. Marinković, S. D. Škapin, P. S. Uskoković, R. R. Aleksić, Polym. Compos., 33 (1) (2012) 22.

[28] W. C. Oliver, G. M. Pharr, J. Mater. Res., 7 (1992) 1564.

[30] F. Söderlind, H. Pedersen, R.M. Petoral Jr. , P. O. Käll , K. Uvdal, J. Collid Interf. Sci., 288 (2005) 140.

[30] S. S. Musbah, V. Radojević, N. Borna, D. Stojanović, M. Dramićanin, A. Marinković, R Aleksić, J. Serb. Chem. Soc., 76 (8) (2011) 1153.

[31] S. C. Tjong, Mater. Sci. Eng. R, 53 (2006) 73.

[32] S. Y. Fu, X. Q. Feng, B. Lauke, Y. W. Mai, Compos. Part B-Eng, 39 (6) (2008) 933.

[33] J. Gearing, K. P. Malik., P. Matejtschuk, Cryobiology, 61 (2010) 27.

[34] P. Alves, J. F. Coelho, J. Haack, A. Rota, A. Bruinink, M. H. Gil, Eur. Polym. J., 45 (2009) 1412.

[35] S. D. Clas, K. Lalonde, K. Khougaz, C. R. Dalton, R. Bilbeisi, J. Pharm. Sci., 101 (2) (2012) 558.

[36] S. Bistac, J. Schultz, Prog. Org. Coat., 31 (4) (1997) 347.

[37] C. Gourgon, J. H. Tortai, F. Lazzarino, C. Perret, G. Micouin, O. Joubert, S. Landis, J. Vac. Sci. Technol., B 22 (2004) 602.

[38] Y. Y. Sun, M. Song, J. Min. Metall. Sect. B-Metall. 48 (1) B (2012) 45.

[39] D. Stojanovic, A. Orlovic, S. Markovic, V. Radmilovic, P. S. Uskokovic, R. Aleksic, J. Mater. Sci., 44 (2009) 6223.

[40] E. Tang, G. Cheng, X. Ma, Powder Technol., 161 (2006) 209.

[41] M. A. Fortin, R. M. Petoral Jr, F. Söderlind, A. Klasson, M. Engström, T. Veres, P. O. Käll, K. Uvdal, Nanotechnology, 18 (2007) 395501.